The Step-Mountain Coordinate: Physical Package

ZAVIŠA I. JANJIĆ*

Institute for Meteorology, Faculty of Physics, Belgrade, Yugoslavia

(Manuscript received 26 June 1989, in final form 22 December 1989)

ABSTRACT

A comprehensive physical package has been developed for a regional eta coordinate model with the steplike mountain representation. This paper describes the basic problems, concepts and numerical techniques developed, and reviews primarily those aspects of the performance of the model which reflect the effects of the parameterized physical processes.

The Level 2.5 turbulence closure model in the Mellor–Yamada hierarchy was chosen to represent the turbulence above the surface layer. A severe instability encountered in the early experiments in the turbulent kinetic energy (TKE) equation was found to be of a numerical origin. The instability was removed by a suitably designed time-differencing scheme. As implemented in the eta-coordinate model, the Level 2.5 turbulence closure model is computationally remarkably inexpensive. An unconditionally stable, trivially implicit, time-differencing scheme is proposed for the vertical diffusion.

The Mellor–Yamada Level 2 turbulence closure scheme is used for the surface layer. For additional flexibility, a shallow logarithmic, dynamical turbulence layer, is introduced at the bottom of the Level 2 surface layer. A rather conventional formulation has been chosen for the ground surface processes and surface hydrology.

The nonlinear fourth order lateral diffusion scheme was implemented in the model. The diffusion coefficient depends on deformation and TKE. The ratio of the horizontal turbulent coefficients for momentum and heat was estimated. The divergence damping is used as another mechanism for maintaining the smoothness of prognostic fields and/or accelerating the geostrophic adjustment.

The Betts and Miller approach has been adopted for deep and shallow cumulus convection. The formulation of the large-scale condensation is rather conventional, and includes the evaporation of precipitating water in the unsaturated layers below the condensation level.

A review of the available results of numerical experiments suggests that the eta model is competitive with other sophisticated models using similar resolutions, and requiring similar computational effort. Thus, it is believed that the viability of the eta coordinate step-mountain approach in grid point models has been finally demonstrated.

1. Introduction

As a generalization of the well-known sigma vertical coordinate (Phillips 1957), Mesinger (1984) proposed the so-called eta coordinate using a step-like mountain representation. A schematic representation of the mountains with this "step-mountain" coordinate is shown in Fig. 1. In the figure, u, T and p_s represent the u component of velocity, temperature and surface pressure, respectively, and N is the maximum number of the eta layers.

In contrast to the sigma coordinate, the coordinate surfaces of the eta coordinate are quasi-horizontal. The steeply sloping coordinate surfaces, and their undesirable effects in the sigma system (pressure gradient force error, advection and lateral diffusion problems) are not likely to be eliminated in the foreseeable future by increasing horizontal resolution. More specifically, higher horizontal resolution generally means steeper and higher mountains, and therefore, further aggravation rather than alleviation of the problem. On the other hand, in addition to the quasi-horizontal coordinate surfaces, the eta coordinate preserves the simplicity of the lower boundary condition of the sigma system. It should be noted that a model using the eta coordinate can be run in the sigma mode, and thus a direct comparison between the two vertical coordinates can be made with an otherwise identical model (Mesinger and Janjić 1987; Mesinger et al. 1988a, hereafter referred to as M$^+$).

In an atmospheric model using the eta coordinate, three major problems can be anticipated:

- Internal boundaries at the vertical sides of the mountain walls,
- Vectorization, and
- Physical package.

* Present affiliation: UCAR visiting scientist at NMC, Washington, D.C.

Corresponding author address: Dr. Zaviša I. Janjić, National Meteorological Center, W/NMC2, WWB, Room 204, Washington, D.C. 20233.

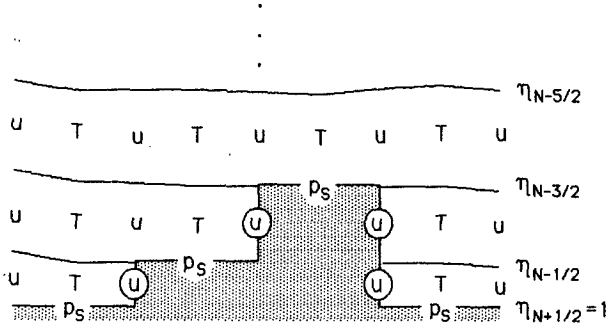

FIG. 1. Schematic representation of a vertical cross section in the eta coordinate using step-like representation of mountains. Symbols u, T and p_s represent the u component of velocity, temperature and surface pressure, respectively. N is the maximum number of the eta layers. The step-mountains are indicated by shading.

The first two were addressed in M$^+$. Namely, they implemented the eta coordinate in the dry, "minimum physics" HIBU (Hydrometeorological Institute and Belgrade University) limited area model. This model will be referred to as the "eta model" in this paper.

The eta model is defined on the semistaggered Arakawa E grid, and uses the technique for preventing grid separation (Mesinger 1973; Janjić 1974) in combination with the split-explicit time-differencing scheme (Mesinger 1974; Janjić 1979). The horizontal advection used in the model has a built-in strict nonlinear energy cascade control (Janjić 1984). The "minimum physics" package consisted of the skin friction, a simple parameterization of the vertical turbulent momentum transport based on simplified mixing length theory, and the dry convective adjustment.

Concerning the internal boundaries, it turned out that the no-slip boundary condition at the vertical mountain walls preserves all major properties of the horizontal discretization. Specifically, the single property not conserved is the E grid momentum, although the conservation of the rotational part of momentum as defined on an equivalent Arakawa C grid is preserved. The term "equivalent C grid" is used here to denote the C grid rotated for an angle of 45°, and with the streamfunction points coinciding with those of the E grid (Janjić 1984; M$^+$). In the term appearing in the continuity equation due to the application of the technique preventing the grid separation, the horizontal fluxes across the mountain walls are set to zero (M$^+$).

The vectorization problems peculiar to the eta coordinate are solved in a straightforward manner, i.e., by using masks set either to 0 or to 1, depending on whether the grid point is inside the mountain or in the free atmosphere. In this way exactly the same computations are performed at all grid points. The model code vectorizes well and executes efficiently.

The "minimum physics" eta model showed considerable skill, both in relative and absolute terms (M$^+$). In several parallel runs, the model run in the eta mode outperformed its sigma mode counterpart. The sigma system runs showed increased noisiness, particularly in temperature fields at higher levels. It was speculated in M$^+$ that this noise was related to the sigma system pressure gradient force error.

The third of the listed problems, that of the physical package, will be addressed in this paper. Designing of a comprehensive physical package is associated with a large number of relatively small problems which together create a big one. In this case, the situation is further complicated by the lack of experience with the step-mountain representation, particularly concerning the treatment of the planetary boundary layer (PBL).

Detailed description of all the problems involved, and the techniques used, is beyond the scope of the present paper. Instead, the emphasis will be placed on the problems and procedures developed for the eta model which may have more general significance. For more details on the eta model physical package, the reader is referred to the documentation prepared by Black (1988), Gerrity and Black (1988) and Lazić and Telenta (1988).

Some of the problems that will be discussed are of numerical origin. Generally speaking, this group of problems has received little attention in scientific literature. It is often believed that parameterization schemes do not require sophisticated numerical treatment because the accuracy of the parameterizations is not as high as that of the equations governing the large-scale atmospheric motions, and therefore, the numerical errors involved can be expected to remain small compared to the errors of the parameterization schemes. In addition, even if the parameterizations were perfect, they introduce strong sources and sinks of energy, so that presumably small spurious sources due to numerical errors can be tolerated. Although generally reasonable, this view may sometimes lead to numerical problems that obscure the physical processes being represented. One such example occurring in the treatment of turbulent processes will be discussed in more detail here.

Concerning the overall performance of the eta model with full physics, the most comprehensive testing, tuning and further refinement have been carried out at NMC Washington, where the model is run on a quasi-operational basis. The eta model has also been implemented in the tropics (Lazić and Telenta 1988; Lazić 1990) and over Europe (Janjić and Lazić 1988; Janjić et al. 1988). The runs in the tropics are believed to be important for testing the convection scheme and convectively driven circulations. The results of the tests performed by other investigators, and published elsewhere, will be briefly reviewed here. Because of anticipated problems with the treatment of PBL with currently used vertical resolution, however, the performance of the parameterizations used for the turbulent processes will be discussed in more detail. The results that will be shown indicate that these parameterizations

are capable of producing turbulent variables that are of the same order of magnitude as those observed, or obtained in PBL simulations, and that these variables show temporal and spatial variations that are consistent with external forcing.

2. Basic concepts and problems

a. Turbulence in the PBL and in the free atmosphere

The Level 2.5 turbulence closure model in Mellor–Yamada hierarchy (Mellor and Yamada 1974, 1982; hereafter referred to as MY74 and MY82, respectively) has been chosen for the treatment of turbulence in the planetary boundary layer (PBL) and in the free atmosphere (cf. Vager and Zilitinkevitch 1968; Zilitinkevitch 1970). This choice was motivated by the theoretical soundness of this closure model, and by its impressive performance in atmospheric models (Miyakoda and Sirutis 1977; Miyakoda et al. 1986).

In spite of this, as well as the fact that the scheme is vectorizable, and therefore, potentially computationally efficient, it has not gained much popularity in leading meteorological centers, where less sophisticated K theories are still predominant. A possible reason for this may be occasional difficulties with this turbulence model (e.g., MY82).

Indeed, in early attempts to implement the Level 2.5 scheme in the eta model, a severe problem was encountered. The turbulent kinetic energy (TKE) was taking on negative or too large values in large parts of the integration domain, leading eventually to computational instability. Of course, an ad hoc technique could be used to keep this pathological feature under control. For example, as is done in some formulations, when negative or too large values are detected, TKE can be modified so as to stay within the prescribed range. Careful examination revealed, however, that the problem was caused by numerical treatment of the TKE production/dissipation term. This problem will be discussed in detail later in the paper, together with the technique developed in order to eliminate it without imposing artificial constraints on TKE itself.

b. The surface layer

The eta coordinate requires rather high vertical resolution in the lower troposphere in order to resolve the mountain steps reasonably well. In addition, it seems desirable to use approximately equidistant eta surfaces in this area, so that the interaction between the atmosphere and the ground surface can be treated approximately equally, both over low-lying and elevated terrain. With presently available computing power and approximately equidistant eta surfaces in the lower troposphere, however, the height of the lowest model level above the underlying surface cannot be expected to be less than about 100–200 m. This is obviously beyond the validity of the Monin–Obukhov similarity theory, which is most frequently used in sigma coordinate models in order to represent the surface layer. For this reason, another approach had to be looked for, preferably such that the turbulent regime within the surface layer is explicitly determined by the vertical derivatives of the large scale variables resolved by the model. The approach that satisfies this requirement is the Level 2 turbulence closure model in the Mellor–Yamada hierarchy (MY74, MY82). Compared to the Level 2.5 model, with this approach the assumption is made that the TKE production and dissipation are exactly balanced. This assumption seems reasonable in the lowest few hundred meters of the atmosphere. As will be discussed in more detail later in the paper, together with the specifics of the Level 2 model implementation, for additional flexibility, a shallow logarithmic dynamical turbulence layer is introduced at the bottom of the Level 2 surface layer. A summary of the methods used for the treatment of turbulent processes in the PBL and in the free atmosphere is schematically represented in Fig. 2.

It should be noted that the Level 2 model is generally comparable in performance with the Monin–Obukhov similarity schemes (cf. MY82). Thus, it can be expected that this scheme will be suitable also for future generations of the eta model using higher vertical resolutions.

c. Surface processes and the exchange of heat with the surface layer

A rather conventional formulation has been chosen for the surface processes (cf. e.g., Miyakoda and Sirutis 1983), with modified treatment of the subsoil processes. The "single-bucket" model is used for ground hydrology, and the heat flux from the surface slab into adjacent soil layers is made proportional to the net radiation at the surface. This method of ground flux specification was generally the second best in Deardorff's (1978) tests. The deep ground temperature flux is estimated using prescribed subsoil temperature at 2.85 m as a function of latitude and terrain elevation. The height of snow is calculated prognostically.

The motivation for such a choice was that the model

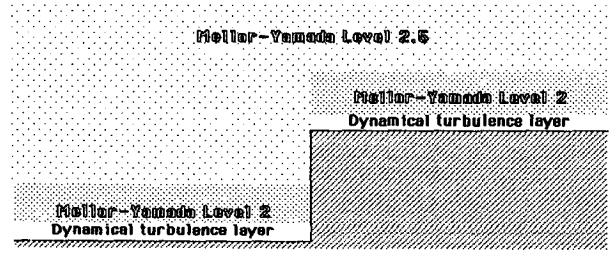

FIG. 2. Illustration of the methods used for the treatment of turbulent processes in the PBL and in the free atmosphere. Cross-hatched shading indicates step-mountains.

was envisaged primarily as an experimental tool which would be used for case studies, including those outside of a well-established operational environment. In such a situation it seems advantageous to minimize the requirements for additional information on surface and subsoil parameters that may be missing or unreliable. Alternatively, due to inertia of the subsoil processes, integrations in the data assimilation mode would be necessary in order to supplement some of the information required by the model.

A problem which is occasionally encountered in atmospheric models (e.g., Kalnay and Kanamitsu 1988) will be also discussed here in the context of the parameterization schemes chosen. This problem is related to the turbulent heat exchange between the soil and the atmosphere and may be due to insufficient time resolution in synoptic scale models. Namely, the observed spectrum of temperature in the surface layer shows a peak for the periods of the order of one to several minutes (e.g., Zilitinkevitch 1970). The time steps used in atmospheric models are typically too long to resolve these oscillations. Thus, for example, if the surface layer becomes very unstable because of radiational heating of the land surface, due to overshooting, too much heat may be transferred into the atmosphere in a single time step, resulting in too cool a land surface and, therefore, too stable a surface layer. This prevents further heat transfer until the land surface is warmed up again so that the next burst of heat can be sent upwards. As will be discussed later in the paper, in order to avoid using too short time steps or a time filtering technique, this process is slowed down in the eta model.

d. Lateral diffusion

The application of lateral diffusion in atmospheric models is somewhat controversial. It is not always clear to what extent this process is needed in order to alleviate the discretization problems. Another issue is how selective the diffusion scheme should be. The second order schemes are often either too damping or insufficiently effective. Following many other modelling groups, the fourth-order nonlinear diffusion has been chosen for the eta coordinate model. As a novelty, however, in addition to deformation, the diffusion coefficient is also made dependent on TKE.

e. Moist processes

For its straightforwardness, simplicity and performance, the Betts and Miller scheme for deep and shallow cumulus convection (Betts 1986; Betts and Miller 1986) has been adopted. Several minor modifications, however, have been introduced. For example, the cloud bottom layer, i.e., the maximum buoyancy level, is searched for through the several lowest model layers above the surface, instead of using just the lowest one. The shallow convective mixing is restricted to a layer that is about 200 hPa deep. Although the shallow convection allowed to operate in deeper layers produced realistically looking precipitation patterns, this has been found to have an adverse effect on the precipitation scores.

Perhaps the most significant early deviation from the original formulation was the treatment of the moist convection in the case of strong buoyancy at low levels and insufficient moisture content in the air column, so that the deep convection was unable to produce positive precipitation. When such a situation occurs, in the original formulation the deep convection is replaced by the shallow one with a rather arbitrarily positioned cloud top. The early experience with the physical package as described here, indicated that it was better to do nothing in such cases, leaving the vertical mixing to be done by the dry turbulent processes. Namely, the shallow convection in the case of insufficient moisture content had a noticeable adverse effect on the precipitation scores. The suspected reason for this was that in combination with other processes, the overall vertical transport of moisture was too efficient.

The formulation of the large-scale condensation is rather conventional. The criterion for the condensation is less than 100% relative humidity in order to allow for partial cloudiness over the grid boxes. In addition, the precipitating water is allowed to evaporate in unsaturated underlying layers until they become saturated, or alternatively, until all of the precipitating water is evaporated.

By tuning the parameters of the convection scheme, and modifying the criterion for the large-scale condensation, the precipitation can be redistributed between the two processes. It is not quite clear, however, what the optimum distribution is.

f. Radiation

The radiation scheme has not been developed independently. Instead, the NMC version of the GLA radiation scheme with interactive random overlap clouds (Davies 1982; Harshvaradhan and Corsetti 1984) has been adapted for application in the eta model by Dr. Thomas L. Black of NMC, Washington, D.C.

3. The Level 2.5 turbulence closure theory: Implementation and the computational problem

a. Governing equations

Before discussing the numerical problems, it is convenient to review the basic features of the physical model used. The Level 2.5 turbulence closure model is governed by the equations (MY82):

$$d(q^2/2)/dt - (\partial/\partial z)[lqS_q(\partial/\partial z)(q^2/2)] = P_s + P_b - \epsilon, \quad (3.1)$$

$$P_s = -\overline{wu}(\partial U/\partial z) - \overline{wv}(\partial V/\partial z),$$

$$P_b = \beta g \overline{w\theta_v}, \quad \epsilon = q^3(B_1 l)^{-1}, \tag{3.2}$$

$$-\overline{wu} = K_M \partial U/\partial z, \quad -\overline{wv} = K_M \partial V/\partial z, \tag{3.3$_1$}$$

$$-\overline{w\theta_v} = K_H \partial \Theta_v/\partial z, \quad -\overline{ws} = K_H \partial S/\partial z, \tag{3.3$_2$}$$

$$K_M = lqS_M, \quad K_H = lqS_H, \tag{3.4}$$

$$S_M(6A_1A_2G_M) + S_H(1 - 3A_2B_2G_H - 12A_1A_2G_H) = A_2, \tag{3.5$_1$}$$

$$S_M(1 + 6A_1^2G_M - 9A_1A_2G_H) - S_H(12A_1^2G_H + 9A_1A_2G_H) = A_1(1 - 3C_1), \tag{3.5$_2$}$$

$$G_M = l^2q^{-2}[(\partial U/\partial z)^2 + (\partial V/\partial z)^2],$$

$$G_H = -l^2q^{-2}\beta g \partial \Theta_v/\partial z. \tag{3.6}$$

Here, S_q, β, A_1, A_2, B_1, B_2, and C_1 are empirical constants (MY82), $q^2/2$ is the turbulent kinetic energy and l is the master length scale yet to be determined. Variables describing the motions resolved by the dynamical part of the model are denoted by capital letters, and the lower case letters are used for turbulent fluctuations. The subscript v is used to denote virtual potential temperature and S is a passive quantity. Note that the specific humidity is considered as a passive quantity within the framework of the model (3.1)–(3.6); the phase changes of the atmospheric water affect the turbulence indirectly, through the changes of the large-scale driving parameters. Here K_M and K_H are the vertical turbulent exchange coefficients for momentum and heat, respectively, and, as indicated by the subscript, P_s and P_b, are the terms describing the production of the turbulent kinetic energy due to shear and buoyancy. The dissipation is denoted by ϵ. Otherwise, the symbols used have their usual meaning. Note that from (3.2), (3.3), (3.4) and (3.6) the contribution of the production/dissipation term may be rewritten in the form

$$P_s + P_b - \epsilon = [S_M G_M + S_H G_H - B_1^{-1}]q^3 l^{-1}. \tag{3.7}$$

Several methods have been proposed for calculating the master length scale l (e.g., Galperin et al. 1988; MY74, MY82; Zilitinkevitch 1970). In the eta model, following MY74 and Miyakoda and Sirutis (1977), the diagnostic formula of the form

$$l = l_0 \kappa z(\kappa z + l_0)^{-1},$$

$$l_0 = \alpha \left[\int_{p_T}^{p_S} |z| q dp\right] \left[\int_{p_T}^{p_S} q dp\right]^{-1}, \tag{3.8}$$

$$\alpha = \text{const}$$

was adopted. Here, p_S and p_T are pressures at the bottom and at the top of the model atmosphere, respectively, κ is the von Kármán constant, and α is an empirical constant. Note that l tends to κz for small z, and to l_0 when z becomes large. The upper limit of about 80 m is imposed on l_0. This value is in agreement with that obtained in high resolution PBL simulations in MY74, MY82.

Having defined the master length scale l by (3.8), G_M and G_H are calculated from (3.6), and S_M and S_H are then readily obtained solving the system (3.5). Now the exchange coefficients for momentum and heat (3.4) can be evaluated, and consequently the turbulent fluxes (3.3), and the forcing terms on the right-hand side of (3.1) can be obtained. It should be mentioned that for exceptionally large shear and/or thermal instability, the system (3.5) may degenerate (MY82) in the sense that its determinant may approach zero. As suggested in MY82, this problem can be eliminated by capping G_M and G_H. Following the general idea of MY82, in the eta model the following constraints are imposed:

$$G_H \leqslant 0.024, \quad G_M \leqslant 0.36 - 15\, G_H. \tag{3.9}$$

Note that the limits (3.9) are more restrictive than those that are really necessary in order to prevent the degeneration of the system (3.5). The motivation for such a choice was to avoid unrealistically large exchange coefficients in the cases of unstable stratification.

b. *Implementation of the Level 2.5 turbulence closure theory*

In the eta model the Level 2.5 scheme is implemented in the "forward–backward" manner. Namely, TKE is updated first, and then the updated values of TKE are used to recalculate the exchange coefficients needed in order to evaluate the contribution of the vertical diffusion. The vertical staggering of the variables and the vertical index are shown in Fig. 3. The symbol eta dot in the figure denotes the vertical velocity in the eta coordinate.

Equation (3.1) is solved in the split mode. Namely, the horizontal and vertical advection, the TKE production and dissipation, and the vertical diffusion are treated in a sequence. Due to vertical staggering, the scheme for horizontal advection has the form

$$\text{Adv}(v, q^2)_{L+1/2} = 0.5[\text{Adv}(v_L, q^2_{L+1/2}) + \text{Adv}(v_{L+1}, q^2_{L+1/2})].$$

The finite-difference operator Adv is an approximation of the continuous horizontal advection operator, v is

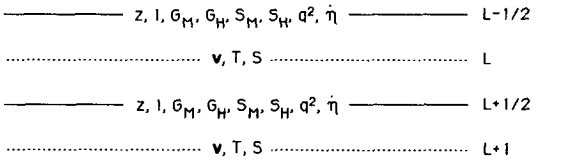

FIG. 3. Schematic representation of the vertical staggering of the variables and the vertical index. The symbol eta dot denotes the vertical velocity in the eta coordinate.

the horizontal velocity and the subscripts denote vertical levels. The advection scheme Adv is analogous to that used for temperature (cf. M+). Using the usual finite-difference notation for two-point differencing and averaging, the scheme for the vertical advection has the form

$$\overline{\overline{\eta}^{\eta}\delta_{\eta}q^{2}}^{\eta}.$$

Although conservative, the advection schemes chosen may produce negative values of TKE. The simplest ad hoc technique is used in the eta model to fix this error. Namely, if detected after the completion of the advection steps, the negative values are replaced by small positive ones. Although spurious TKE sources are introduced in this way, this technique is considered acceptable because, as experience has shown, Eq. (3.1) is strongly dominated by the production/dissipation term.

The production/dissipation terms and the vertical diffusion will be discussed in more detail later. It should be mentioned here, however, that vertical advection and diffusion require vertical boundary conditions. We assume that the turbulent energy vanishes at the top of the model atmosphere, and at the lower boundary, following MY82, the turbulent energy is specified as $B_1^{2/3}u^{*2}$ [cf. Eq. (4.11) later in the text].

c. The computational problem of the Level 2.5 scheme

As already pointed out, in early attempts to implement the Level 2.5 scheme in the eta model, TKE was taking on negative or too large values in large parts of the integration domain, leading eventually to computational instability. Examining the possible causes of the problem, the advection was an obvious first suspect for negative TKE. The experiments, however, showed that the problem would not disappear, even with the advection errors fixed as explained.

The next term inspected was the TKE production and dissipation. As can be seen from (3.7), the contribution of these processes in the split mode may be written in the form

$$\partial(q^2/2)/\partial t = Aq^3,$$

or

$$\partial q/\partial t = Aq^2, \tag{3.10}$$

where

$$A = [S_M G_M + S_H G_H - B_1^{-1}]l^{-1}. \tag{3.11}$$

The expression (3.11) may be either positive or negative, and varies in magnitude depending on the stability and shear, and, in an implicit way through G_M, G_H, and l, on TKE. In the time stepping procedure A will be calculated diagnostically at the beginning of the time step Δt. Thus, if the backward time differencing scheme is used in (3.10) hoping to achieve higher computational efficiency, one obtains

$$q^{\tau+1} = q^{\tau} + A^{\tau}\Delta t(q^{\tau+1})^2.$$

This is a quadratic equation for $q^{\tau+1}$ with the roots

$$q_1{}^{\tau+1} = [1 - (1 - 4A^{\tau}q^{\tau}\Delta t)^{1/2}](2A^{\tau}\Delta t)^{-1}, \tag{3.12}$$

$$q_2{}^{\tau+1} = [1 + (1 - 4A^{\tau}q^{\tau}\Delta t)^{1/2}](2A^{\tau}\Delta t)^{-1}. \tag{3.13}$$

When $\Delta t \to 0$, $q_1{}^{\tau+1} \to q^{\tau}$, and, therefore, q_1 is the physical solution. The other solution is computational and should be damped or removed. Note that q_1 can never be negative since, when $A < 0$, both the numerator and the denominator in (3.12) are negative.

Further inspection reveals, however, that the computational mode is not the only problem. Namely, unless Δt is sufficiently small, the expression under the square root in (3.12) may become negative. Although the maximum time step allowed is difficult to estimate with sufficient accuracy, an idea about its order of magnitude can be obtained from the estimates of A and q. Since A may be both positive and negative, from (3.11) it seems reasonable to assume that it may be of the order of $2/(B_1 l)$. From the simulations (e.g., MY74, MY82) of well developed turbulence, l and q may be assumed to be of the order of 100 m and 2 m s^{-1} respectively. Since $B_1 = 16.6$ (MY82), the expression under the square root in (3.12) will be positive if Δt is less than about 100 s. Of course, there may be exceptional situations requiring even shorter time steps.

The estimate of the maximum time step allowed is rather disappointing since the time steps used in synoptic scale models are typically several times longer. Thus, reducing the time step is likely to make the scheme prohibitively expensive. For this reason, in the eta model an alternative approach is used. Namely, if the time step limitation is locally exceeded, the *growth rate* of the turbulent kinetic energy is limited, i.e., the contribution of the production/dissipation term is calculated from

$$(q^{\tau+1})^2 = [1 - (1 - 4A^{\tau}q^{\tau}\Delta t)^{1/2}]^2(2A^{\tau}q^{\tau}\Delta t)^{-2}(q^{\tau})^2, \quad \text{if} \quad 1 - 4A^{\tau}\Delta t q^{\tau} \geqslant 0, \tag{3.14}_1$$

and

$$(q^{\tau+1})^2 = 4(q^{\tau})^2, \quad \text{if} \quad 1 - 4A^{\tau}\Delta t q^{\tau} < 0. \tag{3.14}_2$$

As can be seen from (3.14), if the time step limitation is exceeded, TKE still quadruples in a single time step. Note that no artificial constraint is imposed on TKE itself.

The technique applied in (3.14) can be compared to commonly used procedures for slowing down processes that are too fast for the time resolution used. Well-known examples of such procedures are polar filtering and implied deceleration of gravity waves associated with the application of the semi-implicit scheme.

The implementation of the described technique was essential in order to get the Level 2.5 scheme working

in the eta model. With this technique, TKE adjusts quickly to the forcing irrespectively of the initial conditions, and behaves well, staying within the bounds expected from physical considerations and high resolution PBL simulations.

4. The surface layer

a. *The Level 2 surface layer with logarithmic extension*

As already mentioned, the "surface layer" of the eta model, i.e., the layer between the ground and the lowest model level, is treated using the Level 2 model in the Mellor–Yamada hierarchy. This model can be derived from the Level 2.5 theory assuming that the TKE production and dissipation are exactly balanced. The governing equations of the Level 2 model are (e.g., MY82):

$$R_f = -P_b/P_s, \tag{4.1}$$

$$R_i = -G_H/G_M = (S_M/S_H)R_f, \tag{4.2}$$

$$S_H = F_1(F_2 - F_3R_f)/(1 - R_f), \tag{4.3}$$

$$S_M = F_4(F_5 - F_6R_f)(F_7 - F_8R_f)^{-1}S_H. \tag{4.4}$$

Here, $F_1, \ldots F_8$ are constants derived from the MY82 constants A_1, A_2, B_1, B_2 and C_1. Since the gradient Richardson number R_i can be calculated from the first of Eqs. (4.2), substituting (4.4) into the second of Eqs. (4.2) and recalculating constants, a quadratic equation is obtained for the flux Richardson number with the root

$$R_f = 0.664[R_i + 0.1765 - (R_i^2 - 0.317R_i + 0.0312)^{1/2}]. \tag{4.5}$$

Note that the constants appearing in (4.5) are different from those of MY74; this is because they were recomputed using the updated values of the constants A_1, A_2, B_1, B_2 and C_1 following MY82.

The turbulent exchange coefficients for momentum and heat are then calculated from [c.f. MY74, Eqs. (66a)–(67b)]

$$K_M = l^2\{[(\partial U/\partial z)^2 + (\partial V/\partial z)^2] \times [B_1(1 - R_f)S_M]\}^{1/2}S_M, \tag{4.6}$$

$$K_H = l^2\{[(\partial U/\partial z)^2 + (\partial V/\partial z)^2] \times [B_1(1 - R_f)S_M]\}^{1/2}S_H. \tag{4.7}$$

Once R_f is computed, S_M and S_H appearing in (4.6) and (4.7) are obtained from (4.3) and (4.4). The length scale l is assumed to vary linearly with z reaching the value of the Level 2.5 master length scale (3.8)–(3.8a) at the top of the lowest model layer.

The shallow "dynamical turbulence layer" at the bottom of the surface layer introduces additional flexibility to the surface layer parameterization. If this layer is sufficiently thin, the ratio of z and the Monin–Obukhov length scale will be small, and therefore logarithmic profiles can be used (e.g., see Zilitinkevitch 1970).

Matching of the level 2 model and the dynamical turbulence layer is schematically represented in Fig. 4. The height of the dynamical turbulence layer is denoted by z_c, z_0 is the roughness height, z_{Lm} is the height of the lowest model level, A, B and C are constants defining the profiles, and α is a meteorological parameter. The subscript s denotes the "surface" value of α, i.e., the value at the height z_0. As can be seen from the figure, a linear profile of α is assumed in between z_c and z_{Lm}. This choice is not based on physical arguments, but rather on the requirement for consistency with the finite-difference approximations used to calculate vertical derivatives in the surface layer. The constants A, B and C are computed from the requirements that α and its first derivative should be continuous at the point z_c, and from the known value of α at the level z_{Lm}.

The vertical derivatives in the surface layer are then approximated by the corresponding value of B, i.e.,

$$\partial\alpha/\partial z \rightarrow B = [\alpha(z_{Lm}) - \alpha_s]/\{z_{Lm} + z_c[\ln(z_c/z_0) - 1]\}. \tag{4.8}$$

The roughness height z_0 is calculated from

$$z_0 = 0.032u^{*2}/g \quad \text{if} \quad 0.032u^{*2}/g \geq 0.0001 \text{ m},$$
$$z_0 = 0.0001 \text{ m} \quad \text{if} \quad 0.032u^{*2}/g < 0.0001 \text{ m} \tag{4.9}$$

over sea, and from

$$z_0 = 0.1 + 0.00001\,\Phi_s \tag{4.10}$$

over land, where Φ_s is the surface geopotential. The friction velocity squared is calculated from

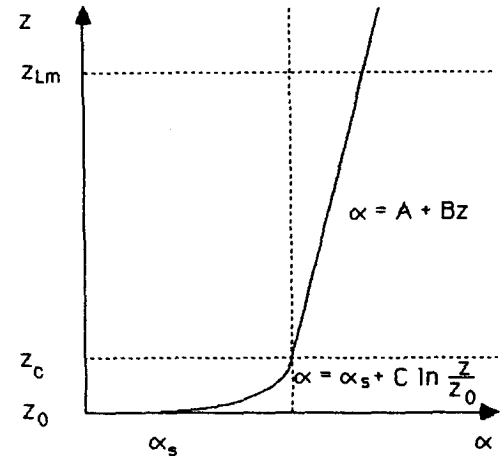

FIG. 4. Schematic representation of matching of the Level 2 model and the logarithmic dynamical turbulence layer. The height of the dynamical turbulence layer is denoted by z_c, z_0 is the roughness height, z_{Lm} is the height of the lowest model level, A, B and C are constants defining the profiles, and α is a meteorological parameter. The subscript s denotes the "surface" value of α, i.e., the value at the height z_0.

$$u^{*2} = \kappa^2 |v(z_c)|^2 / \ln^2(z_c/z_0),$$

or, taking into account the assumptions about the vertical profile shown in Fig. 4,

$$u^{*2} = \kappa^2 z_c^2 |v(z_{Lm})|^2 \times \{z_{Lm} + z_c[\ln(z_c/z_0) - 1]\}^{-2}. \quad (4.11)$$

In (4.11) the value of z_0 from the previous time step is used in order to calculate u^{*2}, and then, z_0 is updated from (4.9).

b. *The surface temperature oscillation*

As already pointed out, the surface temperature oscillation problem may be related to insufficient time resolution in synoptic scale atmospheric models. On the other hand, using short time steps as a remedy would make the parameterization prohibitively expensive. For this reason, Kalnay and Kanamitsu (1988) designed a time-differencing scheme which filters the oscillation so that sufficiently long time steps can be used.

In an attempt to be consistent with the basic modelling philosophy, instead of using a filtering procedure, in the eta model the process is slowed down to the point where the time resolution chosen becomes adequate. In this respect, the choice of the depth of the surface soil layer d_s played the primary role. The criterion for choosing d_s was to make the thermal capacity of the slab comparable to that of the adjacent layer of the air with which the slab is exchanging heat. For moderately wet soils, in the eta model this is achieved with $d_s = 0.1$ m. Note that this value is about twice that used by Miyakoda and Sirutis (1983). With currently used vertical resolution, however, the depth of the lowest eta layer is about 300 m, which is about twice the depth of their lowest layer.

It should be noted that several other available devices may alleviate the problem. Namely, in an unstable surface layer, the dominating term in the surface temperature equation is the turbulent transport of heat. The cooling of the surface slab will be reduced if the turbulent heat flux into the atmosphere is reduced, and the formulation of the surface layer (4.1)–(4.11) offers several possibilities in this respect. As can be seen from (4.8), one of these is to increase the depth of the dynamical turbulence layer z_c; however, there is a limit on z_c beyond which the assumptions about the logarithmic profiles cease to be valid. This limit is of the order of several meters (e.g., Monin and Obukhov 1954) and the value most frequently used in the eta formulation is 2 m. For $z_{Lm} \approx 150$ m, from (4.8) and (4.10), it follows that over land the turbulent fluxes are reduced by about 2.5% due to the presence of the dynamical turbulence layer.

Another possibility is to reduce the exchange coefficient K_H, either by a suitable choice of the length scale l in (4.6)–(4.7), or by setting a limit for R_f in the case of unstable stratification. Of course, the values chosen must not produce unrealistic values of the exchange coefficients.

5. Vertical and horizontal diffusion

a. *Vertical diffusion*

In large-scale atmospheric models vertical resolutions have been reached where, unless very short time steps are used, the simplest forward time differencing applied for vertical diffusion becomes unstable. For this reason, the usual approach is to use the implicit, backward scheme, which is unconditionally stable. Solving the tridiagonal system obtained in this way requires two passes in the vertical. In the eta model an even simpler scheme is employed, i.e.,

$$(A_L^{\tau+1} - A_L^{\tau})/\Delta t = [K_{L-1/2}(A_{L-1}^{\tau} - A_L^{\tau+1})/(z_{L-1} - z_L) - K_{L+1/2}(A_L^{\tau+1} - A_{L+1}^{\tau})/(z_L - z_{L+1})]/(z_{L-1/2} - z_{L+1/2}). \quad (5.1)$$

Note that the only value of the variable A at the time level $\tau + 1$ is located at the vertical level L, and therefore (5.1) can be solved for $A_L^{\tau+1}$. Thus, being trivially implicit, the scheme (5.1) is easy to implement and vectorize.

In order to examine the properties of the scheme, it is convenient to simplify Eq. (5.1). Let the exchange coefficients and the height increments appearing in (5.1) be constant. Then

$$A_L^{\tau+1} = A_L^{\tau} + K\Delta t/(\Delta z)^2 [A_{L-1}^{\tau} + A_{L+1}^{\tau} - 2A_L^{\tau+1}]. \quad (5.2)$$

Substituting into (5.2) the solution of the form $A^{\tau} = \hat{A}\lambda^{\tau} e^{imz}$, where $\hat{A}$ is a complex amplitude, and defining $\mu = K\Delta t/(\Delta z)^2$, and $Z = m\Delta z/2$, we find that

$$\lambda = 1 - 4\mu \sin^2 Z/(1 + 2\mu), \quad (5.3)$$

i.e., the scheme is unconditionally stable since the absolute value of the second term on the right-hand side of (5.3) is always less than 2. However, unlike with the backward scheme, λ may be negative if μ is too large, and undesired phase changes may occur. As a safeguard against these phase changes, the scheme is applied in two consecutive time iterations. Thus, if an erroneous phase change is produced in the first iteration, it will be corrected in the second.

In order to assess how likely the erroneous phase changes are, let us consider a numerical example. Let us assume that $\Delta t = 480$ s, $\Delta z = 350$ m, and $\sin^2 Z = 1$. Let the exchange coefficient K equal 100 $m^2 s^{-1}$, which is close to the maximum values observed in the atmosphere above the surface layer (e.g., cf. Zilitinkevitch 1970), or obtained in high resolution PBL simulations (e.g., MY74, MY82). With these values, $\lambda = 0.12$, i.e., the phase change still does not occur. Of course, if higher vertical resolutions and/or longer time

steps are used, so that λ becomes negative and approaches -1, more than two iterations with smaller time steps can be applied in order to speed up the damping.

b. Lateral diffusion and divergence damping

In spite of the considerable attention that the representation of the lateral diffusion has received, this is still one of the unresolved problems in synoptic scale models. In the absence of a complete and consistent theory, following many other modelers, a rather heuristic approach has been chosen.

The exchange coefficient of the second-order diffusion operator for momentum is defined by

$$K_{M,h} = Cd_{\min}|\Delta|,$$

where C is a constant, $d_{\min}$ is the minimum grid distance, and Δ is proportional to deformation (cf. Smagorinsky 1963; Miyakoda and Sirutis 1983) modified by the presence of the TKE term, i.e.,

$$|\Delta| = [2(\Delta_x u - \Delta_y v)^2 + 2(\Delta_y u + \Delta_x v)^2 + 2C'q^2/2]^{1/2}.$$

The operator Δ followed by a subscript denotes the difference between two neighboring values along the coordinate axis indicated by the subscript. The orientation of the coordinate axes used to define the lateral diffusion operators on the E grid are shown schematically in Fig. 5. Here C' is an empirical constant, and the constraint is imposed on $|\Delta|$ such that

$$|\Delta|_{\min} \leqslant |\Delta| \leqslant |\Delta|_{\max},$$

where the upper and the lower bounds are empirical. The TKE term is included in order to take into account the effects of horizontal mixing due to dry convective entrainment and detrainment. [Subsequent to the decision to include the TKE term, the author became aware that an analogous approach has been taken by Lilly (1962) and Xu (1988) for the convection problem].

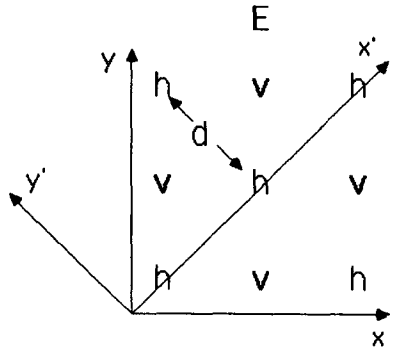

FIG. 5. Schematic representation of the E grid and the orientations of the coordinate axes used to define the second-order lateral diffusion operators. The grid distance d is also indicated.

Another problem is that of the relation between the exchange coefficient for momentum $K_{M,h}$ and that for heat and moisture $K_{H,h}$. In the eta model this relation is estimated by analogy with the Mellor–Yamada Level 2 model. Namely, since there is no buoyancy effect, the analogs of R_i and R_f vanish, and, from (4.1)–(4.4) we find that $S_M/S_H \approx .8$. Consequently, we assume that

$$K_{H,h} = 1.25K_{M,h}. \tag{5.4}$$

Note that the constant appearing in (5.4) is half of the constant quoted by Miyakoda and Sirutis (1983).

Thus, the second-order lateral mixing is represented by the operators

$$D_M(u; v) = (Cd_{\min}/\Delta A_{\text{box}})\{\Delta_{x'}[\overline{|\Delta|^{y'}}\Delta_{x'}(u; v)] + \Delta_{y'}[\overline{|\Delta|^{x'}}\Delta_{y'}(u; v)]\},$$

$$D_H(T; q) = 1.25(Cd_{\min}/\Delta A_{\text{box}}) \times \{\Delta_{x'}[\overline{|\Delta|^{x'}}\Delta_{x'}(T; q)] + \Delta_{y'}[\overline{|\Delta|^{y'}}\Delta_{y'}(T; q)]\}. \tag{5.5}$$

Here, the overbars represent the simplest two-point averaging along the axes indicated by the accompanying superscripts, and ΔA_{box} is the grid box area. The fluxes across the mountain walls are set to zero.

The fourth-order lateral mixing used in the model is computed by repeated application of the second-order operators (5.5). With the present "standard" horizontal resolution of the eta model, the fourth-order lateral diffusion coefficient used in the context of the described formulation does not exceed the order of 10^{13} s^{-1}. For comparison, the coefficients used in global models at the major centers are typically of the order of 10^{15} s^{-1}, i.e., for two orders of magnitude larger. The difference of about one order of magnitude can be explained by higher resolution used in the eta model.

In order to accelerate the geostrophic adjustment process, the lateral diffusion is assisted by rather strong additional divergence damping.

6. Review of the model performance

The eta model and its interfaces with the environments in which it is run have been under constant development. For this reason, the results discussed here should be considered as preliminary. Nevertheless, on the basis of accumulated evidence, a general picture is emerging of what the eta model can do.

a. The integration domain, resolution, computational efficiency and coding

The model has been implemented in three different geographical regions: North America, Europe and tropical regions of Australia. The "standard" resolution used in most runs is 80 km in the horizontal, and 16 or 15 layers in the vertical. The model atmosphere ex-

tends up to 100 hPa. The depths of the layers slowly increase from the ground up to the middle of the atmosphere, and then decrease as the top of the model atmosphere is being approached. The time steps used with this horizontal resolution are typically 4 min for the gravity–inertia terms, 8 min for the advection and large-scale precipitation, and 16 min for the rest of the parameterization schemes. In the North American region, the NMC products are used in order to specify the initial and boundary conditions. In the tropics, the model uses the ECMWF data, while over Europe the ECMWF surface parameters and boundary conditions are combined with analyses produced by the Yugoslav weather service.

With the 80 km resolution, the model has about 8500 grid points in the horizontal in the North American region. Excluding preprocessing and postprocessing, the model requires about 500 CPU seconds per day on the CYBER 205. Out of these, the dynamical part takes about 180 CPU seconds, the physical package excluding radiation about 120 CPU seconds, and the radiation takes about 200 seconds. It is interesting to note that the Level 2.5 turbulence closure model is computationally remarkably inexpensive. It required less CPU time than the previously used dry convective adjustment and a very simple turbulent momentum transport scheme.

In order to ensure easy portability, the model code was written following to the maximum possible extent the standard ANSI FORTRAN 77. The model is kept in core (logically). Where the application of the standard FORTRAN would be too expensive, the CYBER 205 vector processing dialect is used. At such places, however, alternative code in the standard FORTRAN is also provided. This does not apply to the radiation routine, which was entirely written in the CYBER 205 dialect. So far, the model has been implemented on machines of four different manufacturers (CYBER 205, Cray, IBM, DEC). A scalar version of the radiation routine is used on machines other than CYBER 205.

b. Turbulent variables

The examples presented here were produced in a 48 hour North American run starting on 22 August 1989 at 1200 UTC. The model had 16 layers in the vertical, and the horizontal resolution was 80 km. The boundary conditions were derived from the global aviation forecast of the U.S. National Weather Service starting 12 hours earlier. The initial conditions were obtained by interpolation from the initialized fields.

An example demonstrating the temporal and spatial variation of the model produced TKE at a constant eta surface is shown in Fig. 6. The level chosen is the interface between the thirteenth and fourteenth (from top) eta layer. This interface is located at about 885 hPa. Due to rather large spatial variation of TKE, the isolines of $\log_{10}q^2$ are actually drawn. The dashed contours correspond to the negative values, and the shaded area represent the volume blocked by the mountains. The 12 hour (upper left panel) and 36 hour (lower left panel) forecast times correspond to late afternoons, and the 24 hour (upper right panel) and 48 hour (lower right panel) forecast times correspond to early mornings. As can be seen from the figure, the turbulent energy responds well to the diurnal cycle, reaching maximum values of the order of 1 $m^2 s^{-2}$ in the afternoons, and decreasing to generally much lower levels in the mornings. Note that the values over large water surfaces are low at this level at all forecast times.

Figure 7 shows a vertical cross section of $\log_{10}q^2$. The cross section extends from 26°N, 96°W to 55°N, 87°W and the values plotted correspond to the 36 hour forecast. The shaded steps represent the model topography, and the numbers along the vertical axis indicate the model layers. In the lower troposphere the depth of the layers is increasing with height and varies from about 300 to about 500 meters. Lighter shading in the leftmost part of the diagram indicates the sea surface. As before, the dashed contours correspond to the negative values of $\log_{10}q^2$. As can be seen from the figure, the maximum values of the turbulent energy are of the order 1 $m^2 s^{-2}$, and are found in the range of about 300–800 m above the ground, which is in a reasonably good qualitative agreement with the results obtained in high resolution PBL simulations (MY74, MY82).

Finally, Fig. 8 displays $\log_{10}$ of matched Level 2 and Level 2.5 heat exchange coefficients on the same cross section, and for the same forecast time as in Fig. 7. As can be seen from the figure, in the late afternoon the exchange coefficients reach the order of 100 $m^2 s^{-1}$ in sunny regions over land. These values are of the same order of magnitude as those observed, or obtained in high resolution PBL simulations under similar conditions (cf. e.g., Zilitinkevitch 1970; MY74; MY82).

c. A review of recent studies on the performance of the model

The most comprehensive testing, tuning and further development of the eta model and its interfaces with the environment have been carried out at NMC Washington, where the model is run on a quasi-operational basis. The recent results of these activities have been summarized by Mesinger and Black (1989) and Black and Mesinger (1989). In their studies, special attention was paid to precipitation as an important prognostic variable which is perhaps most difficult to predict accurately. In the period considered (November 1988), the eta model generally had a considerable advantage over the operational NMC regional precipitation forecasts produced by a sophisticated model with comparable resolution over the North America and adjacent waters, and requiring about the same computational effort. The eta model threat scores were better for accumulated 24 hour rainfall amounts of 0.50 inches and

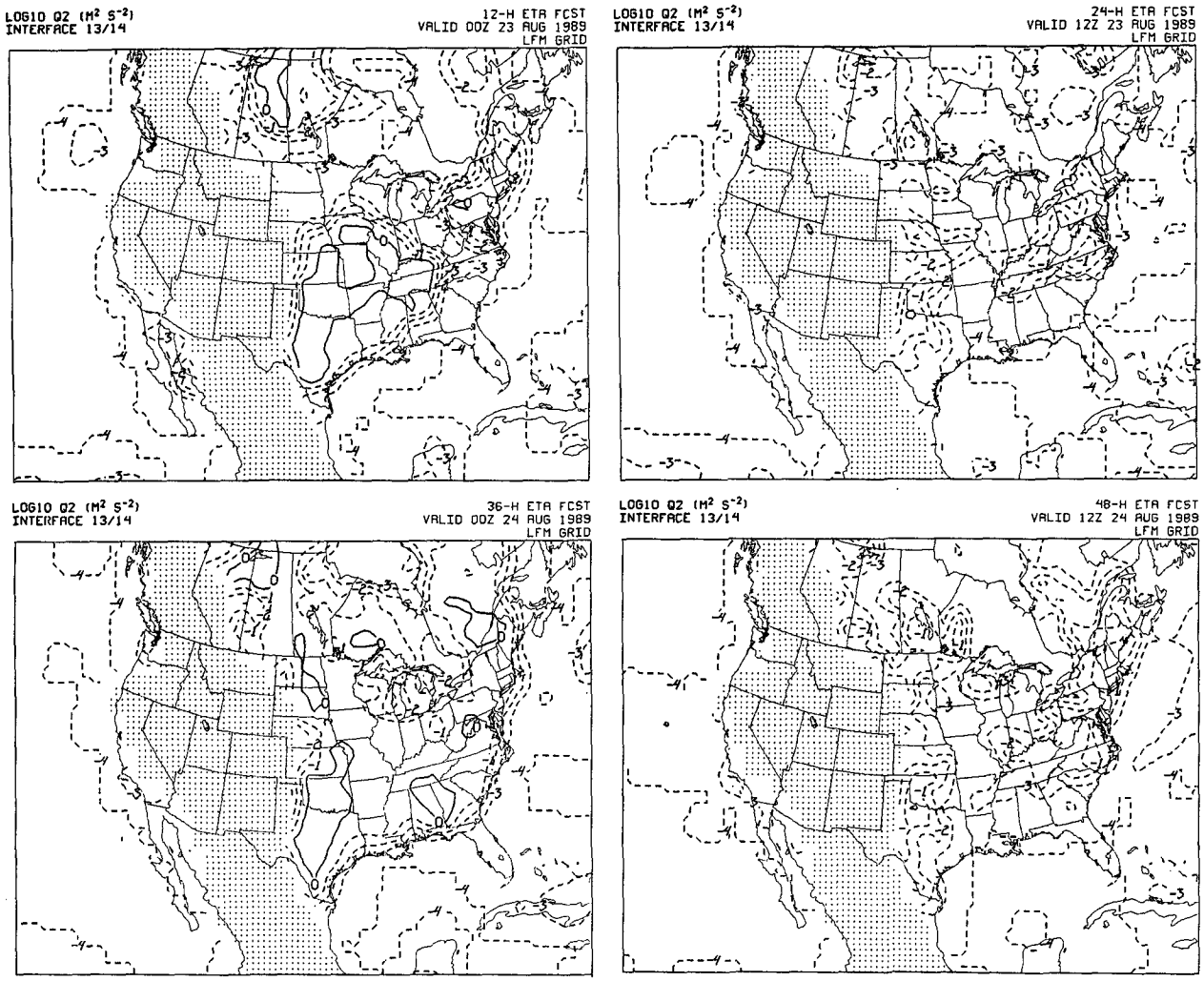

FIG. 6. Contour of $\log_{10} q^2$ (q^2 in $m^2\ s^{-2}$) at a constant eta surface. The fields shown correspond to: 12 hour (upper left panel), 24 hour (upper right panel), 36 hour (lower left panel) and 48 hour (lower right panel) forecast times. The dashed contours correspond to negative values of $\log_{10} q^2$. The shaded area represent the volume blocked by the mountains.

more. The improvements reached about a factor of 2 for the 1.25 and 1.50 inch categories. These improvements did not arise as a result of forecasting more than observed amounts of intense precipitation. In fact, the bias scores showed that both models underpredicted heavier amounts of precipitation, but the eta model noticeably less so than the other model. At the 500 hPa level, the eta model also had smaller mean height error, standard deviation height error and the total rms error.

Concerning the synoptic features, an overall impression was that the main advantage of the eta model over the current operational NMC regional forecasting system were improved predictions of major storm systems (e.g., WGNE 1988; Mesinger and Black 1989; Black and Mesinger 1989).

A notably difficult forecast to which particular attention has been given, both in the early stages of the eta model development (M+), and in the runs with the full physics (Black and Janjić 1988), is that of Appalachian redevelopment of 28 March 1984 accompanied by severe weather and tornado outbreak (cf. Kocin et al. 1984; Collins and Tracton 1985; Gyakum and Barker 1988). This case was rerun using twice the standard horizontal resolution, i.e., 40 km (Mesinger et al. 1988b). Perhaps the most notable feature produced in this run was the 36 hour forecast of accumulated 24 hour precipitation. Compared to already in many respects encouraging forecast obtained with the standard resolution (Black and Janjić 1988), the double resolution precipitation pattern was surprisingly detailed, and in a remarkably good general agreement with the observations. This suggests that the eta model possesses the ability to improve with increased horizontal resolution. At these resolutions this feature is not always taken for granted.

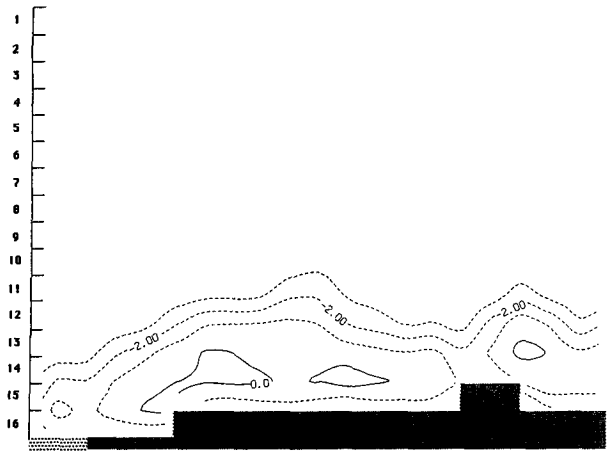

FIG. 7. Vertical cross section of $\log_{10}q^2$ (q^2 in $m^2 s^{-2}$) at 36 hours extending from 26°N 96°W to 55°N 87°W. The shaded steps represent the model topography. Model layers are indicated along the vertical axis. Lighter shading on the left indicates the sea surface. The dashed contours correspond to negative values of $\log_{10}q^2$.

As an additional refinement of the physical package, a viscous sublayer (e.g., Zilitinkevitch 1970; Pielke 1984) has been recently introduced next to the surface (Black and Mesinger 1989). Due to potentially reduced heat and moisture transfer resulting from the presence of this sublayer, its incorporation into the model was accompanied by a return to the conventional use of the Betts convection scheme (Betts 1986; Betts and Miller 1986), in the sense that the shallow convection is performed in the situations when insufficient moisture content in vertical columns prevents the deep convection to produce positive precipitation. A considerable improvement of an east coast storm forecast was reported with these modifications (Black and Mesinger 1989).

As already pointed out, the eta model has also been implemented in the tropics (Lazić and Telenta 1988). This is believed to be important for testing the convection scheme and convectively driven circulations. The model was tested in 48 hour simulations of the tropical cyclones Connie, Irma, Damien and Jason (Lazić 1989) from the Australian Monsoon Experiment (AMEX) period. The initialized (then) operational ECMWF analyses were used to specify the initial conditions, and the boundary conditions were derived from the archived ECMWF forecasts. For the analyses only the real-time GTS data were available, excluding the delayed mode AMEX data. From the synoptic point of view, the results were considered as remarkably good under the circumstances, both in absolute terms, and compared to the results obtained with other models (Lazić and Telenta 1988; Lazić 1990). In particular, the model showed the ability to predict the genesis of Irma. The forecasts also compared favorably with the ECMWF operational products (communicated by Lazić). Of course, since the eta model had higher horizontal resolution, this result cannot be considered as relevant for intercomparison of the two models. It indicates, however, the benefits that one might expect from the application of regional models in order to refine the global forecasts.

7. Conclusions

In an atmospheric model using the step-mountain eta coordinate, three major problems can be anticipated: (1) the internal boundaries at the vertical sides of the mountain walls, (2) vectorization and (3) the physical package. The first two were addressed, and successfully solved, by Mesinger et al. (1988a). The third one, that of the physical package, is discussed in this paper.

In the case of the eta coordinate, design of a comprehensive physical package is complicated by the lack of experience with the step-like mountain representation, particularly concerning the representation of PBL. The Level 2.5 turbulence closure model in the Mellor–Yamada hierarchy (Mellor and Yamada 1974, 1982; cf. Vager and Zilitinkevitch 1968; Zilitinkevitch 1970) was chosen to represent the turbulence above the surface layer. The model was implemented using time-splitting. In early experiments, however, a severe problem was encountered: TKE was taking on too large or negative values in large parts of the integration domain, leading eventually to numerical instability. The problem was found to be of numerical origin, and related to the treatment of the TKE production/dissipation term. A suitably designed time-differencing scheme eliminated this problem. With this scheme, TKE adjusts quickly to the forcing irrespectively of the initial conditions, and behaves well, staying within the bounds expected from physical considerations and high resolution PBL simulations. Except for rather insignificant errors produced in the advection step, no artificial con-

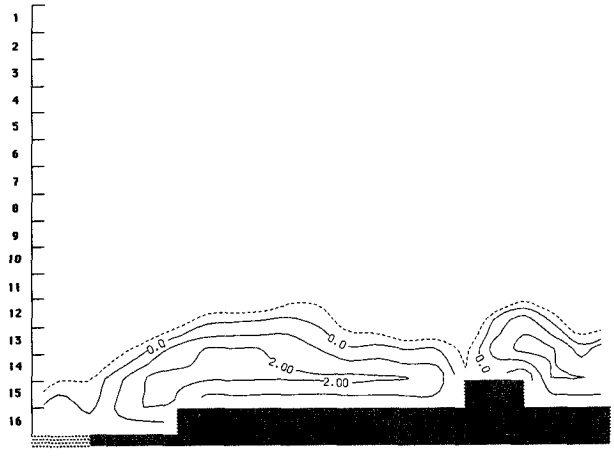

FIG. 8. Vertical cross section as in Fig. 7, but for $\log_{10}$ of matched Level 2 and Level 2.5 heat exchange coefficients (in $m^2 s^{-1}$).

straints are imposed on TKE itself. As implemented in the eta-coordinate model, the Level 2.5 turbulence closure model is computationally remarkably inexpensive.

A trivially implicit time-differencing scheme was designed for vertical diffusion. The scheme is unconditionally stable and easily vectorizable.

With presently available computing power, the height of the lowest eta model level above the underlying surface is of the order of 100–200 m, which is beyond the validity of the Monin–Obukhov similarity theory. Although this problem is likely to be alleviated, or even disappear, in the next generation models using higher vertical resolutions, the Mellor–Yamada Level 2 turbulence closure scheme (Mellor and Yamada 1974, 1982) has been chosen for the surface layer. With this scheme, the TKE production and dissipation are assumed to be exactly balanced, and the turbulent regime within the surface layer is explicitly determined by the vertical derivatives of the large scale variables resolved by the model. For additional flexibility, a shallow logarithmic, dynamical turbulence layer, is introduced at the bottom of the Level 2 surface layer.

Rather conventional formulation has been chosen for the ground surface processes and surface hydrology (cf. e.g., Miyakoda and Sirutis 1983). The possible intermittent turbulent transports in the surface layer under unstable conditions are prevented by choosing the depth of the surface layer of soil in such a way that its heat capacity become comparable to that of the adjacent layer of the air.

Following many other modeling groups, the fourth order nonlinear lateral diffusion has been chosen for the eta coordinate model. The diffusion coefficient depends on deformation (cf. Smagorinsky 1963; Miyakoda and Sirutis 1983) and TKE (cf. Lilly 1962; Xu 1988). The ratio of the turbulent coefficients for momentum and heat exchanges was estimated by analogy with the Mellor–Yamada Level 2 model. The fourth-order diffusion coefficients are constrained not to exceed values that are about two orders of magnitude smaller than those typically used in global models at the major centers; an approximately one order of magnitude smaller coefficient would be required on account of the smaller grid distance. However, rather strong divergence damping assists the lateral diffusion in maintaining the smoothness of prognostic fields and/or accelerating the geostrophic adjustment process.

With several minor modifications, the Betts and Miller approach has been adopted for deep and shallow cumulus convection (Betts 1986; Betts and Miller 1986). The formulation of the large-scale condensation is rather conventional, and includes the evaporation of precipitating water in the unsaturated layers below the condensation level.

The radiation scheme has not been developed independently. Instead, the NMC version of the GLA radiation scheme with interactive random overlap clouds (Davies 1982; Harshvaradhan and Corsetti 1984) has been adapted for application in the eta model.

A review of the results of numerical experiments (Janjić and Black 1987; Black and Janjić 1988; Mesinger et al. 1988b; Mesinger and Black 1989; Black and Mesinger 1989; Lazić and Telenta 1988; Lazić 1990) suggests that the eta model is competitive with other sophisticated regional models using similar resolutions, and requiring about the same computational effort. In the experiments, no obvious major problem has been identified which could be related with certainty to possible deficiencies in the basic formulations of the parameterization schemes. Moreover, the eta model showed ability to improve with the horizontal resolution increased to about 40 km, which is not always taken for granted. Thus, one may conclude that the performance of the physical package is not below the present standards. At the same time, the flexibility of the parameterizations allow further tuning and refinements. Contemplating further developments, two obvious candidates for upgrading are surface and subsoil processes, and large scale precipitation.

Summarizing, of the three major anticipated eta coordinate problems, all three appear to have satisfactory solutions. Thus, it is believed that the viability of the eta coordinate in grid point models has been finally demonstrated.

Acknowledgments. This research was supported by the University Corporation for Atmospheric Research under Contract 9523. The physical package was developed and implemented in the eta model while the author was visiting NMC Washington in 1987. All results presented here, and most of those referred to, were produced using the NMC databases and computer facilities. The author is indebted to Dr. Thomas L. Black for designing the radiation driver and modifying the radiation routine for application in the eta model, as well as for handling the interfaces with the NMC data archives, graphics and data reformatting, reinterpolations and conversions. On several occasions, his careful reading of the code saved the time that would otherwise be lost on debugging. His suggestions on the model parameters to be looked at facilitated early identification and elimination of several problems. Good advice, and previously developed interfaces for the eta model by Dr. Dennis Deaven were highly appreciated. The author had the privilege of numerous productive discussions with Drs. Jim Hoke, Jim Tucillo and Geoff DiMego. Implementation and coding of the convection scheme was greatly facilitated by references to the code obtained from Joe Sela. The precipitation verification routines used in the tests were made available by Dr. John Ward. The author enjoyed the support of the late Dr. John Brown and Drs. Eugenia Kalnay and Joe Gerrity. The author's visit was made possible to a large extent by the personal engagement of Dr. Ron Mc-

Pherson. The author also wishes to thank numerous other people he contacted during the visit and had productive discussions with, and to whom perhaps injustice is done by not mentioning them by name. In the early planning and decision making period, and in the preparation of the paper, the author had the support of the Serbian Academy of Sciences and Arts, Association for Science of Serbia and Yugoslav Federal Fund for Fostering Science and Technology. The author is also grateful for lengthy and valuable discussions with Dr. Bora Rajković of Belgrade University on the Mellor–Yamada hierarchy of turbulence closure models, and to Dr. Martin Miller of ECMWF on convection schemes. These discussions influenced the choices of the schemes used in the eta model. Many contacts and useful suggestions by Prof. Fedor Mesinger helped to finalize and improve the text of this paper. In addition, the author is grateful for the most efficient and effective handling of a number of practical problems to Ms. Meg Austin, Ms. Sandi Bell and Ms. Gina Taberski of UCAR, and to Ms. Carolyn Hodge of NMC.

REFERENCES

Betts, A. K., 1986: A new convective adjustment scheme. Part I: Observational and theoretical basis. *Quart. J. Roy. Meteor. Soc.*, **112,** 677–691.

——, and M. J. Miller, 1986: A new convective adjustment scheme. Part II: Single column tests using GATE wave, BOMEX, ATEX and Arctic air-mass data sets. *Quart. J. Roy. Meteor. Soc.*, **112,** 693–709.

Black, T. L., 1988: The step-mountain, eta coordinate regional model: A documentation. NOAA/NWS/NMC Washington, 47 pp. [NOAA/NWS/NMC Washington, Development Division, W/NMC2, WWB, Room 204, Washington, DC 20233.]

——, and Z. I. Janjić, 1988: Preliminary forecast results from a step-mountain eta coordinate regional model. *Eighth Conf. on Numerical Weather Prediction,* Baltimore, Amer. Meteor. Soc., 442–447.

——, and F. Mesinger, 1989: Forecast performance of NMC's eta coordinate regional model. *12th Conf. on Weather Analysis and Forecasting,* Monterey, Amer. Meteor. Soc., 551–555.

Collins, W. G., and M. S. Tracton, 1985: Evaluation of NMC's regional analysis and forecast system-heavy precipitation events. Preprints, *Sixth Conf. on Hydrometeorology,* Indianapolis, Amer. Meteor. Soc., 289–296.

Davies, R., 1982: Documentation of the solar radiation parameterization in the GLAS climate model. NASA Tech. Memo. 93961, 57 pp. [NASA/Goddard Space Flight Center, Greenbelt, MD 20771.]

Deardorff, J., 1978: Efficient prediction of ground temperature and moisture with inclusion of a layer of vegetation. *J. Geophys. Res.*, **83,** 1989–1903.

Emanuel, K. A., 1988: Reply. *J. Atmos. Sci.*, **45,** 3528–3530.

Galperin, B., L. H. Kantha, S. Hassid and A. Rosati, 1988: A quasi-equilibrium turbulent energy model for geophysical flows. *J. Atmos. Sci.*, **45,** 55–62.

Gerrity, J. P., and T. L. Black, 1987: Exposition of the HIBU model formulation of the turbulent transfer process. NOAA/NWS/NMC Washington, 14 pp. [NOAA/NWS/NMC Washington, Development Division, W/NMC2, WWB, Room 204, Washington, DC 20233.]

Gyakum, J. R., and E. S. Barker, 1988: A case study of explosive subsynoptic scale cyclogenesis. *Mon. Wea. Rev.*, **116,** 2225–2253.

Harshvardhan, and D. G. Corsetti, 1984: Longwave radiation parameterization for the UCLA/GLAS GCM. NASA Tech. Memo. 86072, 48 pp. [NASA/Goddard Spece Flight Center, Greenbelt, MD 20771.]

Janjić, Z. I., 1974: A stable centered difference scheme free of two-grid-interval noise. *Mon. Wea. Rev.*, **102,** 319–323.

——, 1979: Forward-backward scheme modified to prevent two-grid-interval noise and its application in sigma coordinate models. *Contrib. Atmos. Phys.*, **52,** 69–84.

——, 1984: Nonlinear advection schemes and energy cascade on semistaggered grids. *Mon. Wea. Rev.*, **112,** 1234–1245.

——, and T. L. Black, 1987: Physical package for the step-mountain, eta coordinate model. *Research Activities in Atmospheric and Oceanic Modelling,* WCRP, No. 10, 5.24–5.26.

——, and L. Lazić, 1988: Feasibility study on the application of the HIBU model with included physical package (excluding radiation) into the operational practice of FHMI. Tech. Rept., Dept. Meteor., University of Belgrade, 20 pp. (in Serbo-Croatian). [Institute for Meteorology, Faculty of Physics, P.O. Box 550, YU-11001 Belgrade, Yugoslavia.]

——, T. L. Black, L. Lazić and F. Mesinger, 1988: Forecast sensitivity to the choice of the vertical coordinate. *Annales Geophysicae*—special issue devoted to the XIII General Assembly of the European Geophysical Society, Bologna, 147.

Kalnay, E., and M. Kanamitsu, 1988: Time schemes for strongly nonlinear damping equations. *Mon. Wea. Rev.*, **116,** 1945–1958.

Kocin, P. J., L. W. Uccellini, J. W. Zack and M. L. Kaplan, 1984: Recent examples of mesoscale numerical forecast of severe weather events along the East Coast. NASA Tech. Memo. TM 86172, 57 pp. [NASA/Goddard Space Flight Center, Greenbelt, MD 20771.]

Lazić, L., 1990: Forecasts of AMEX tropical cyclones with step-mountain model. *Aust. Met. Mag.*, in press. [Author's address: Institute for Meteorology, Faculty of Physics, P.O.B. 550, YU-11001 Belgrade, Yugoslavia.]

——, and B. Telenta, 1988: UB/NMC Eta Model (documentation). *WMO, Tropical Meteorology Programme,* 303 pp.

Lilly, D. K., 1962: On the numerical simulation of buoyant convection. *Tellus,* **14,** 148–172.

Mellor, G. L., and T. Yamada, 1974: A hierarchy of turbulence closure models for planetary boundary layers. *J. Atmos. Sci.*, **31,** 1791–1806.

——, and ——, 1982: Development of a turbulence closure model for geophysical fluid problems. *Rev. Geophys. Space Phys.*, **20,** 851–875.

Mesinger, F., 1973: A method for construction of second-order accuracy difference schemes permitting no false two-grid-interval wave in the height field. *Tellus,* **25,** 444–458.

——, 1974: An economical explicit scheme which inherently prevents the false two-grid-interval wave in the forecast fields. *Proc. Symp. on Difference and Spectral Methods for Atmosphere and Ocean Dynamics Problems,* Novosibirsk, Acad. Sci., Novosibirsk, Part II, 18–34.

——, 1984: A blocking technique for representation of mountains in atmospheric models. *Riv. Meteor. Aeronautica,* **44,** 195–202.

——, and Z. I. Janjić, 1987: Numerical technique for the representation of mountains. *Observation, Theory and Modelling of Orographic Effects, Seminar 1986, Vol. 2,* ECMWF, Reading, England, 29–80.

——, and T. L. Black, 1989: Verification tests of the eta model, October–November 1988. *NMC Office Note 355,* 47 pp. [NOAA/NWS/NMC, Development Division, W/NMC2, WWB, Room 204, Washington, DC 20233.]

——, Z. I. Janjić, S. Ničković, D. Gavrilov and D. G. Deaven, 1988a: The step-mountain coordinate: Model description and performance for cases of Alpine lee cyclogenesis and for a case of an Appalachian redevelopment. *Mon. Wea. Rev.*, **116,** 1493–1518.

——, T. L. Black and Z. I. Janjić, 1988b: A summary of the NMC step-mountain (ETA) coordinate model. *Proc. Workshop on Limited-area Modeling Intercomparison,* Boulder, NCAR, 91–

98. [Mesoscale and Microscale Meteorology Division, NCAR, P.O. Box 3000, Boulder, CO 80307.]

Miyakoda, K., and J. Sirutis, 1977: Comparative integrations of global models with various parameterized processes of subgrid-scale vertical transports: Description of the parameterizations. *Contrib. Atmos. Phys.*, **50,** 445–587.

——, and ——, 1983: Impact of sub-grid scale parameterizations on monthly forecasts. *Proc. ECMWF Workshop on Convection in Large-Scale Models,* ECMWF, Reading, England, 231–277.

——, —— and J. Ploshay, 1986: One-month forecast experiments—without anomaly boundary forcing. *Mon. Wea. Rev.*, **114,** 2363–2401.

Monin, A. S., and A. M. Obukhov, 1954: Basic laws of turbulent mixing in the surface layer of the atmosphere. *Contrib. Geophys. Inst. Acad. Sci. USSR,* **151,** 163–187 (in Russian).

Phillips, N. A., 1957: A coordinate system having some special advantages for numerical forecasting. *J. Meteor.*, **14,** 184–185.

Pielke, R. A., 1984: *Mesoscale Meteorological Modeling.* Academic Press, 612 pp.

Smagorinsky, J., 1963: General circulation experiments with the primitive equations. Part I: The basic experiment. *Mon. Wea. Rev.*, **91,** 99–164.

Vager, B. G., and S. S. Zilitinkevitch, 1968: Theoretical model of diurnal variations of meteorological fields. *Meteorology and Hydrology,* No. 7, 3–18 (in Russian).

WGNE, 1989: Rep. of the fourth session of the CAS/JSC Working Group on Numerical Experimentation. Downsview, Ontario, Canada, WMO/TD-No. 278, 76 pp.

Xu, Q., 1988: A formula for eddy viscosity in the presence of moist symmetric instability. *J. Atmos. Sci.*, **45,** 5–8.

Zilitinkevitch, S. S., 1970: Dynamics of the planetary boundary layer. *Gidrometeorologicheskoe Izdatelystvo, Leningrad,* 292 pp. (in Russian).